Metabolic Engineering 14 (2012) 611–622

Contents lists available at SciVerse ScienceDirect

Metabolic Engineering

journal homepage: www.elsevier.com/locate/ymben

Xylose isomerase overexpression along with engineering of the pentose phosphate pathway and evolutionary engineering enable rapid xylose utilization and ethanol production by *Saccharomyces cerevisiae*

Hang Zhou [a], Jing-sheng Cheng [a], Benjamin L. Wang [a], Gerald R. Fink [b], Gregory Stephanopoulos [a,*]

[a] Department of Chemical Engineering, Massachusetts Institute of Technology, Room 56-469, 77 Massachusetts Avenue, Cambridge, MA 02139, United States
[b] Whitehead Institute for Biomedical Research, 9 Cambridge Center, Cambridge, MA 02142, United States

ARTICLE INFO

Article history:
Received 22 February 2012
Received in revised form
10 July 2012
Accepted 21 July 2012
Available online 16 August 2012

Keywords:
Xylose isomerase
Saccharomyces cerevisiae
Evolutionary engineering
Inverse metabolic engineering
Xylose utilization
Ethanol production

ABSTRACT

Xylose is the main pentose and second most abundant sugar in lignocellulosic feedstocks. To improve xylose utilization, necessary for the cost-effective bioconversion of lignocellulose, several metabolic engineering approaches have been employed in the yeast *Saccharomyces cerevisiae*. In this study, we describe the rational metabolic engineering of a *S. cerevisiae* strain, including overexpression of the *Piromyces* xylose isomerase gene (*XYLA*), *Pichia stipitis* xylulose kinase (*XYL3*) and genes of the non-oxidative pentose phosphate pathway (PPP). This engineered strain (H131-A3) was used to initialize a three-stage process of evolutionary engineering, through first aerobic and anaerobic sequential batch cultivation followed by growth in a xylose-limited chemostat. The evolved strain H131-A3-AL^{CS} displayed significantly increased anaerobic growth rate ($0.203 \pm 0.006\ h^{-1}$) and xylose consumption rate ($1.866\ g\ g^{-1}\ h^{-1}$) along with high ethanol conversion yield (0.41 g/g). These figures exceed by a significant margin any other performance metrics on xylose utilization and ethanol production by *S. cerevisiae* reported to-date. Further inverse metabolic engineering based on functional complementation suggested that efficient xylose assimilation is attributed, in part, to the elevated expression level of xylose isomerase, which was accomplished through the multiple-copy integration of *XYLA* in the chromosome of the evolved strain.

1. Introduction

Use of renewable biomass for the production of transport fuels is becoming increasingly important due to the decreasing fossil energy resources and growing concerns about climate change. Cost-effective production of cellulosic bio-ethanol is dependent on complete and fast utilization of lignocellulosic biomass. Although the broadly used fermentative yeast *Saccharomyces cerevisiae* is one of the most effective ethanol-producing organisms from hexose sugars, it does not naturally ferment pentose D-xylose, the second most abundant sugar in lignocellulosic biomass after glucose. Consequently, *S. cerevisiae* has been extensively engineered to incorporate an efficient D-xylose assimilation pathway (Hahn-Hägerdal et al., 2007; Maris et al., 2007; Van Vleet and Jeffries, 2009).

The conversion of xylose to xylulose can be mediated via two different pathways. Most xylose-utilizing eukaryotes convert xylose into xylulose in a two-step redox reaction, catalyzed by the predominantly NADPH-dependent xylose reductase (XR) followed by the NAD^+-dependent xylitol dehydrogenase (XDH), with xylitol as the pathway intermediate (Jeffries, 1983). Recombinant *S. cerevisiae* strains expressing these enzymes can ferment xylose to ethanol, however, under anaerobic conditions, the different coenzyme specificities of XR and XDH generate a cofactor imbalance which results in considerable xylitol accumulation as a by-product and reduces the yield of ethanol (Bruinenberg et al., 1983; Hahn-Hägerdal et al., 2007).

In the second pathway, the isomerization of xylose to xylulose is catalyzed by the metal-ion-dependent enzyme xylose isomerase (XI). The XI pathway eliminates the cofactor imbalance and accompanying excessive production of xylitol. A number of bacterial *XYLA* genes coding for XIs have been heterologously expressed in *S. cerevisiae*, including *XYLA* from *Escherichia coli* (Sarthy et al., 1987), *Clostridium thermosulfurogenes* (Moes et al., 1996), *Bacillus subtilis* or *Actinoplanes missouriensis* (Amore et al., 1989), *Thermus thermophilus* (Walfridsson et al., 1996) and *Streptomyces rubiginosus* (Gardonyi and Hahn-Hägerdal, 2003). Nevertheless, all the attempts were unsuccessful until XI from the anaerobic fungus *Piromyces* (Kuyper et al., 2003; Kuyper et al., 2005a; Maris et al., 2007) and *Orpinomyces* (Madhavan et al., 2009a; Madhavan et al., 2009b) were functionally

* Corresponding author. Fax: +1 617 253 3122.
E-mail address: gregstep@mit.edu (G. Stephanopoulos).

1096-7176/$ - see front matter © 2012 Elsevier Inc. All rights reserved.
http://dx.doi.org/10.1016/j.ymben.2012.07.011

expressed at high levels in *S. cerevisiae*. The first bacterial XI from *Clostridium phytofermentans* was also expressed in *S. cerevisiae*, and the bacterial XI is reported to be less susceptible to inhibition by xylitol than is the enzyme from the Piromyces strain (Brat et al., 2009).

D-Xylulose is subsequently phosphorylated to D-xylulose-5-phosphate (X5P) by xylulokinase (XK), and channeled through the pentose phosphate pathway (PPP) to glycolysis. To facilitate high flux of xylose assimilation, XK including either the endogenous *S. cerevisiae XKS1* (Ho et al., 1998; Johansson et al., 2001; Toivari et al., 2001) or the *Pichia stipitis XYL3* (Jin et al., 2003) were also overexpressed, along with the genes of the non-oxidative PPP (*RPE1*, *RKI1*, *TKL1*, and *TAL1*) (Jin et al., 2005; Johansson and Hahn-Hägerdal, 2002; Karhumaa et al., 2005; Kuyper et al., 2005a). Still, the heterologous expression of these genes by themselves was not sufficient for efficient utilization of xylose. The problem was finally overcome by evolutionary engineering, a method that has been extensively used and proven to be very effective in obtaining *S. cerevisiae* strains with improved fermentation performance on xylose (Kuyper et al., 2005b; Pitkänen et al., 2005; Sauer, 2001; Sonderegger and Sauer, 2003), arabinose (Becker and Boles, 2003) or co-utilization of D-xylose and L-arabinose (Karhumaa et al., 2006; Rosa et al., 2010; Wiedemann and Boles, 2008). Furthermore, successful genetic analysis of an evolved strain can identify useful genotypes aiding in further rational engineering (Nevoigt, 2008).

Table 1
Plasmids used in this study.

Plasmids	Characteristics	Reference
pRS404	YIp, *TRP1*	Sikorski and Hieter (1989)
pRS405	YIp, *LEU2*	Sikorski and Hieter (1989)
pRS416GPD	CEN, *URA3*, *TDH3*p-MCS-*CYC1*t	Mumberg et al. (1995)
pRS415	CEN, *LEU2*	Mumberg et al. (1995)
pRS415-geno	Genomic library of H131-A3^{SB-3}	This study
pRS404-*RKI1-RPE1*	*TRP1*, *TDH3*p-*RKI1-CYC1*t, *TDH3*p-*RPE1-CYC1*t	This study
pUCHI2-*TKL1*	pUC19, *Hind*III-*HIS2-Hind*III, *HIS2*, *TDH3*p-*TKL1-CYC1*t	This study
pUCAD2-*PsTAL1*	pUC19, *Hind*III-*ADH1-Hind*III, *TDH3*p-*PsTAL1-CYC1*t	This study
pUCAR1-*PsXYL3*	pUC19, *Hind*III-*ARG4-Hind*III, *ARG4*, *HXT7*p-*PsXYL3-CYC1*t	This study
pRS426-*XYLA*	2μ ori, *URA3*, *TDH3*p-*XYLA-CYC1*t	This study
pRS426-*XYLA-XYL3*	2μ ori, *URA3*, *TDH3*p-*XYLA-CYC1*t, *TDH3*p-*PsXYL3-CYC1*t	This study
pRS406-$(XYLA)_2$	*URA3*, 2 copies of *HXT7p-XYLA-CYC1t* in tandem	This study

In the present paper, we report on a metabolic engineering study to improve xylose fermentation by a *S. cerevisiae* strain. The key genes for the xylose metabolic pathway, *Piromyces XYLA* and *P. stipitis XYL3*, were introduced to enable xylose utilization. In addition, the genes for PPP were overexpressed to overcome other potential limitations of xylose assimilation. Sequential batch cultivation followed by cultivation in a xylose-limited chemostat with increasing dilution rate was finally used to select for strains with improved growth and xylose consumption rate. The fermentation performance of the constructed and evolved yeast strains was evaluated yielding one isolate, H131-A3^{SB-3}, with very high rates of growth, xylose assimilation and ethanol production. An inversed metabolic engineering based on functional complementation was deployed to discover the dominant genotype of the rapid xylose-fermenting strain.

2. Materials and methods

2.1. Strains and maintenance

Yeast strains used in this study are summarized in Table 2. Yeast and bacterial strains were stored in 15% glycerol at −80 °C. *E. coli* and grown in Luria–Bertani medium. Ampicillin (50 mg/L) was added to the medium when required. Yeast strains were routinely cultivated at 30 °C in YNB (6.7 g/L yeast nitrogen base without amino acids; Becton, Dickinson and Company, MD, USA), plus 20 g/L of glucose (YNBG) or xylose (YNBX) and a mixture of appropriate nucleotides and amino acids. For growth on plates, cells were grown on SD medium (Synthetic Defined medium, contains YNB and a Complete Supplement Mixture of amino acids with appropriate dropout, Sunrise Science Products, Inc., San Diego, CA) with glucose or xylose.

2.2. Construction of plasmids and xylose-utilizing strains

Plasmids used in this study are summarized in Table 1. All *S. cerevisiae* strains were constructed from BF264-15Dau (Table 2, kindly provided by Gerald R. Fink, Whitehead Institute). In order to express the genes of the non-oxidative PPP, the endogenous *RPE1*, *RKI1*, *TKL1* and *P. stipitis TAL1* genes were amplified from *S. cerevisiae* or *P. stipitis* genomic DNA using appropriate primers (Table 3) and cloned into integration plasmids, each with the glyceraldehydes-3-phosphate dehydrogenase promoter (*TDH3p*). The constructed yeast integration plasmids pRS404-*RKI1-RPE1*, pUCAD2-*PsTAL1* and pUCHI2-*TKL1* were then linearized by proper restriction enzyme and transformed to BF264-15Dau sequentially to yield the PPP overexpression background strain H131 (*MATa*, *TRP1::TDH3p-RKI1-CYC1t-TDH3p-RPE1-CYC1t*, *HIS2::TDH3p-TKL1-CYC1t*, *ADE1::TDH3p-PsTAL1-CYC1t*, *leu2*, *ura3*, *arg4*).

Table 2
S. cerevisiae strains used in this study.

S. cerevisiae strains	Characteristics	Reference
BF264-15Dau	MATa, *ade1*, *his2*, *leu2-3,112*, *trp1-1*, *ura3*, *arg4*	Sun et al. (1989)
H131	BF264-15Dau, *TRP1::TDH3p-RKI1-CYC1t-TDH3p-RPE1-CYC1t*, *HIS2::TDH3p-TKL1-CYC1t*, *ADE1::TDH3p-PsTAL1-CYC1t*	This study
H131-A3	H131 (pRS426-*XYLA-XYL3*)	This study
H131-A3^{SB-1}	Single-colony isolate of strain H131-A3, evolved after aerobic sequential batch cultivation	This study
H131-A3^{SB-2}	Single-colony isolate of strain H131-A3^{SB-1}, evolved after micro-aerobic sequential batch cultivation	This study
H131-A3^{SB-3}	Single-colony isolate of strain H131-A3^{SB-2}, evolved after anaerobic sequential batch cultivation	This study
H131-A3^{CS}	Single-colony isolate of strain H131-A3^{SB-3}, evolved after chemostat	This study
H131-A3-AL^{CS}	H131-A3^{CS}, *arg4* complemented by pUCAR1 containing *ARG4*, *leu2-3*complemented by pRS405 containing *LEU2*	This study
H132	H131, *ARG4::HXT7p-PsXYL3-CYC1t*	This study
H132-A	H132[pRS406-$(XYLA)_2$]	This study
H132-A^{SB}	Single-colony isolate of strain H132-A, evolved after aerobic sequential batch cultivation	This study

Table 3
Primers used in this study.

Oligo name	Sequence
RPE1-F-Spe I	AAAAACTAGTATGGTCAAACCAATTATAGC
RPE1-R-Xho I	ATACTCGAGCTAATCTAGCAAATCTCTAGAA
RKI1-F-Xba I	ATTATCTAGAATGGCTGCCGGTGTCCCAA
RKI1-R-Xho I	ATAACTCGAGTCACTTTTCGGTAACTTCA
TKL1-F-Xba I	ATTATCTAGAATGACTCAATTCACTGACAT
TKL1-R Xho I	ATATCTCGAGTTAGAAAGCTTTTTTCAAAGG
PsTAL1-F-Spe I	GGACTAGTATGTCCTCCAACTCCCTTGA
PsTAL1-R-Xho I	TACTCGAGTTAGAATCTGGCTTCCAATTGT
PsXYL3-F-Spe I	AAGTTTACTAGTAAAATGACCACTACCCCATTTG
PsXYL3-R-Xho I	TTCTCGAGTTAGTGTTTCAATTCACTTTCCATCTT
XYLA-F-Xba I	AATCTAGAATGGCTAAAGAGTACTTCCCA
XYLA-R-Xho I	TTCTCGAGTTATTGATACATTGCGACAATAG
PsXYL3-F-Spe I	AAGTTTACTAGTAAAATGACCACTACCCCATTTG
PsXYL3-R-Xho I	TTCTCGAGTTAGTGTTTCAATTCACTTTCCATCTT

Underline indicates restriction recognition sites.

For the xylose metabolic pathway, the *XYLA* from *Piromyces* sp. E2 was codon optimized (synthesized by GenScript, Piscataway, NJ 08854) and cloned to the multiple-copy vector pRS426GPD to yield pRS426-*XYLA*. In order to increase the activity of xylulokinase, the *XYL3* gene from *P. stipitis* was expressed in addition to the endogenous *XKS1*. The *PsXYL3* was amplified from *P. stipitis* genome and inserted into pRS426-*XYLA* behind a *TDH3* promoter, resulting in pRS426-*XYLA-XYL3*. H131 was finally transformed with pRS426-*XYLA-XYL3* to generate strain H131-A3.

2.3. Shake flask cultivation

For growth rate measurements, cells were grown in 50 mL of YNBX medium in a 250 mL Erlenmeyer flask shaken at 200 rpm. Sponge plugs were used for aerobic growth and rubber stoppers (with a 23G1 syringe needle to release CO_2 during fermentation) were used for anaerobic growth. Initial cell growth was used for calculation of the specific growth rate. Sequential batch cultivation was carried out under similar aerobic or anaerobic condition in YNBX or SDX (SD+20 g/L xylose) medium, once the culture reached stationary phase an inoculum was taken to start a new batch at OD_{600} of 0.05.

2.4. Chemostat cultivation

Anaerobic chemostat cultivation was carried out at 30 °C in 500 mL Water Jacketed Spinner Flasks (Bellco Glass, Vineland, NJ) with a fixed working volume of 200 mL, using a leveled effluent driven by a peristaltic pump. Cultures were grown in YNBX medium at various xylose concentrations. After inoculation and completion of the batch phase, chemostat cultivation was initiated by feeding YNBX to the fermentor at increasing dilution rates. The initial dilution rate (0.02 h^{-1}) was increased stepwise once the culture reached a steady state. Cultures were stirred at 250 rpm. pH was monitored but not maintained. The effluent broth was examined periodically by microscopic to verify the absence of contamination.

2.5. Anaerobic fermentation of xylose

For the characterization of the engineered and evolved strains, pre-cultures were grown in YNBX. A first pre-culture (5 mL in 14 mL BD Falcon Round-Bottomed Tube) grown overnight aerobically was used to inoculate a second 50 mL inoculum in a plugged 250 mL flask. Cells from late exponential phase were harvested, washed twice with fresh YNBX medium and inoculated at 0.05 g DCW/L. Fermentation was conducted in 1.3 l BioFlo 110 bioreactors (New Brunswick Scientific, Edison, NJ) with 1 L of 2 × YNBX supplemented with 40 g/L xylose. Temperature was controlled at 30 °C and agitation was controlled at 200 rpm. pH was maintained at 5.0 by automatic addition of 4 N NaOH. Nitrogen was sparged before inoculation. The medium was supplemented with the anaerobic growth factors ergosterol (0.01 g/L) and Tween 80 (0.42 g/L) dissolved in ethanol in 1000 × to characterize the finally evolved strain, H131-A3-AL^{CS}, under anaerobic conditions.

2.6. Determination of metabolites and culture dry weight

Glucose, xylose, xylitol, organic acids, glycerol and ethanol were detected by a Waters Alliance 2695 HPLC (Waters, Milford, MA) with a Waters 410 Differential Refractometer and a Bio-Rad HPX-87H column (Bio-Rad, Hercules, CA). The column was eluted at 50 °C with 14 mM of sulfuric acid at a flow rate of 0.7 mL/min.

For dry cell weight, culture samples (10.0 mL) were filtered with preweighed cellulose acetate syringe filters (diameter 25 mm, pore size 0.2 μm; VWR, Batavia, IL). After filtration of the broth, the cells were washed twice with de-ionized water, dried in a microwave oven for 15 min at 500 W and weighed. The measurements of dry cell weight were repeated and the variation is less than 2%. The maximum specific growth rates were calculated from the initial exponential growth phase. The average consumption rates of xylose, production rates of ethanol as well as the yields of ethanol and xylitol were calculated from the growth phase (from the beginning of fermentation to about 10 g/L residual xylose).

2.7. Construction of genomic library

Genomic DNA was isolated from the target *S. cerevisiae* strain, and partially digested with restriction enzyme *Sau3A* I. Then, DNA fragments at the size of 3–8 kbp were isolated from an agarose gel after electrophoresis, and purified again with ethanol precipitation. Shuttle vector pRS415 (Mumberg et al., 1995) was used as the backbone and digested with *Sal* I. Both the genomic DNA fragments and the digested vector were treated with the DNA polymerase I Klenow Fragment (3′→5′ exo-) and the appropriate dNTPs, in order to reduce the 5′ overhang length from four nucleotides to two nucleotides to avoid self-ligation of the vector as well as ligation among genomic DNA fragments. After ligation of the fragments and the backbone by T4 ligase, the resulting plasmids were transformed into ElectroMAX DH5α-E (*Invitrogen*) and plated on agar petri-dishes with ampicillin. This colony-forming unit (CFU) was counted and plasmid was mini-prepped for analysis and transformation of yeast.

2.8. Enzymes, primers and chemicals

Restriction enzymes, polymerase, DNA-modifying enzymes and other molecular reagents were obtained from New England Biolabs (Beverly, MA). Reaction conditions were as recommended by the supplier. All general chemicals were purchased from Sigma (St. Louis, MO) unless otherwise stated. Synthesized primers for PCR and sequencing were purchased from Invitrogen (Carlsbad, CA). Qiaprep spin miniprep Kit (Qiagen, Valencia, CA) was used for *E. coli* plasmid extraction. Frozen-EZ Yeast Transformation II Kit (Zymo Research) or similar lithium acetate yeast transformation protocol were used for yeast transformation.

2.9. Quantitative PCR for gene copy numbers

The copy numbers of genes *XYLA* and *PsXYL3* were determined through quantitative PCR (Bieche et al., 1998; Jin et al., 2003). Endogenous *PGK1* was used as reference during the quantification.

Genomic DNA was isolated using Promega Wizard Genomic DNA Purification Kit (Promega, Madison, WI). The concentration and purity of DNA was determined using a NanoDrop 1000 Spectrophotometer (Thermo Scientific, West Palm Beach, FL). Quantitative PCR was performed using a Bio-Rad iCycler iQ Real-Time PCR Detection System and iQ SYBR Green Supermix (Bio-Rad, Hercules, CA). Quantitative PCR conditions were as recommended by the supplier: 400 nM of each primer was used in one step of 95 °C for 3 min, and 40 cycles of 95 °C for 10 s, 55 °C for 15 s and 72 °C for 15 s. Endogenous *PGK1* was used as a reference to quantify the copy number of *XYLA* and *XYL3*. 12.8, 3.2, 0.8, 0.2, and 0.05 ng of DNA template was used.

2.10. Genome-wide expression analysis

Yeast OneArray Hybridization Service (PhalanxBio Inc., Belmont, CA) was used to monitor mRNA transcripts of putative *S. cerevisiae* open reading frames. Microarray analysis was performed in triplicate. Microarray data were processed in the EXPANDER (EXpression Analyzer and DisplayER) 5.2 (Ulitsky et al., 2010). Differentially expressed genes from evolutionarily engineered strains on glucose or xylose fermentation were selected using two criteria: (1) those for which $p<0.05$ in *t*-tests (FDR control was used for multiple testing correction) performed on samples and (2) those that showed more than a twofold change. All differentially expressed genes in each fermentation process were sorted into 10 clusters using the *K*-Means method according to gene expression patterns. Functional enrichment of genes in each cluster was explored using EXPANDER 5.2. Information about specific gene functions and biological pathways was obtained from the Saccharomyces Genome Database (http://www.yeastgenome.org).

Quantitative RT-PCR was used to measure the expression of *XYLA*, *PsXYL3* and *PsTAL1* transcripts. Total RNA from yeast cells was isolated using the RNeasy Mini Kit (Qiagen). Quantitative RT-PCR analysis was carried out using the iScript One-Step RT-PCR Kit with SYBR Green (Bio-Rad). *PGK1* was used as a reference and 10, 1, 0.1 and 0.01 ng of total RNA template was used. All reactions were performed in triplicate. All kits were used under conditions recommended by the supplier.

2.11.XI and XK activity assay

Saccharomyces cerevisiae was grown to the exponential phase in YNBG or YNBX medium. Cells were harvested by centrifugation for 10 min at 8000 × *g* and 4 °C. The pellet was washed twice with chilled washing buffer (10 mM phosphate buffer, 2 mM EDTA, pH 7.5) and suspended in chilled extraction buffer (100 mM phosphate buffer, 2 mM $MgCl_2$, 1 mM dithiothreitol, pH 7.5). The suspended cells were mixed with 0.5 mM glass beads (Sigma), vortexed at maximum rate for 1 min, and then cooled on ice for 1 min. This procedure was repeated for up to 10 min. The glass beads and cellular debris were removed by centrifugation for 15 min at 15,000 × *g* and 4 °C. The crude extract (supernatant) was collected and used for the enzyme assay. Total protein concentration in cell extracts was determined using the Pierce Coomassie Protein Assay Reagent Kit (Pierce Biotechnology, Rockford, IL) with bovine serum albumin as the standard.

Xylose isomerase activity in cell extracts was determined spectrophotometrically using a method modified from Kerstershilderson et al. (1987): the assay mixture (1 mL) containing 100 mM Tris–HCl buffer (pH 7.5), 10 mM $MgCl_2$, 0.2 mM NADH, 2 U sorbitol dehydrogenase (Roche, Mannheim, Germany) and 20 μL of cell extract was equilibrated at 30 °C for 5 min. The reaction was started by the addition of D-xylose to a final concentration of 200 mM. The assay was performed at 30 °C for 10 min using a Ultrospec 2100 pro UV/Visible Spectrophotometer (GE Healthcare Biosciences, Pittsburgh, PA). An extinction coefficient at 340 nm of NADH of 6.3 $mM^{-1}cm^{-1}$ was used to calculate the specific activity. One unit of xylose isomerase activity was defined as the amount of enzyme required to produce 1 μM of xylulose per min under the assay conditions.

Xylulokinase activity was measured according to the method of Shamanna and Sanderson (1979). The assay mixture (1 mL) containing 20 mM Tris–HCl (pH 7.5), 2 mM ATP, 0.2 mM PEP, 3 mM glutathione, 0.1 mM NADH, 2 mM $MgCl_2$, 5 mM KCN (NADH oxidase inhibitor), 5 mM NaF (ATPase inhibitor), 150 mg/L LDH-PK (~30 U for each enzyme), and 20 μL cell extract was equilibrated at 30 °C for 5 min. The reaction was started by the addition of D-xylulose to a final concentration of 2 mM. One unit of xylulokinase activity is defined as the amount of enzyme that phosphorylates 1 μmol of xylulose per minute under the assay conditions.

2.12.Pulsed field gel electrophoresis (PFGE) and chromosome blot

Chromosomal DNA was prepared as described by Carle and Olson (1985). Chromosomes were separated on a 1% agarose gel (Bio-Rad) in a 0.5 × TBE buffer at 6V/cm at 14 °C, using a Bio-Rad CHEF-DIII mapper apparatus. The following migration conditions were used: a pulse time of 60 s for 15 h and a pulse time of 90 s for 9 h at an angle of 120°. The gel was stained with ethidium bromide to identify the chromosomal DNA. [32P]dCTP-labeled DNA probes were prepared using the Prime-It II Random Primer Labeling Kit (Stratagene, La Jolla, CA). Blotting results were analyzed using the software ImageJ (NIH).

3. Results

3.1. Construction of xylose-utilizing strains

Several plasmids were constructed to integrate the genes of the non-oxidative PPP. In order to express the endogenous *RPE1*, *RKI1*, *TKL1* and *P. stipitis TAL1* genes under the strong constitutive glyceraldehydes-3-phosphate dehydrogenase promoter (*TDH3p*), the genes were amplified from *S. cerevisiae* or *P.* stipitis genomic DNA using appropriate primers (Table 3) and integrated to the genome of BF264-15Dau (Table 2), resulting in the pentose phosphate pathway overexpression strain H131 (Table 2. *MATa*, *TRP1::TDH3p-RKI1-CYC1t-TDH3p-RPE1-CYC1t*, *HIS2::TDH3p-TKL1-CYC1t*, *ADE1::TDH3p-PsTAL1-CYC1t*, *leu2*, *ura3*, *arg4*).

H131 was then transformed with multi-copy plasmid pRS426-*XYLA-XYL3* to generate strain H131-A3, which contains a complete xylose metabolic pathway. Following transformation, a single colony was isolated from SD plate with glucose. The specific growth rate of H131-A3 on SDX liquid medium was 0.031 ± 0.022, under aerobic condition (Table 4).

The basic xylose assimilation pathway was engineered in the initial strain that was used to initiate the evolution process. This included overexpression of xylose isomerase–xylulose kinase along with several PPP genes including transaldolase (*TAL1*) from *P. stipitis* that has been shown to be superior to *S. cerevisiae*. As such, overexpression of *PsTAL1* did not cause growth inhibition when cells were grown on glucose, unlike that of the *S. cerevisiae TAL1* (Jin et al., 2005). Similarly, *XYL3* from *P. stipitis* was used instead of *XKS1* from *S. cerevisiae*, due to its higher activity (Jin et al., 2003) and better substrate specificity to xylulose (Akinterinwa and Cirino, 2009).

3.2. Xylose assimilation and ethanol production are significantly improved by evolutionary engineering

The engineered *S. cerevisiae* strain H131-A3 (Table 2) that overexpresses *Piromyces XYLA*, *P. stipitis XYL3* and genes in PPP

Table 4
Characteristics and fermentation performance of xylose-fermenting *S. cerevisiae* strains.

Strain	Description	Conditions	Yields (g/g)		Ethanol production[a] ($g\,g^{-1}\,h^{-1}$)	Xylose consumption[a] ($g\,g^{-1}\,h^{-1}$)	μ_{max} (h^{-1})	Reference
			Ethanol	Xylitol				
H131-A3	*XYLA*, *PsXYL3*, *PsTAL1*, *TKL1*, *RPE1*, *RKI1*	Aerobic batch, SDX 2% xylose	N/A	N/A	N/A	N/A	0.031 ± 0.022	This study
H131-A3^{SB-1}	Selection of H131-A3, aerobic sequential batch	Aerobic batch, SDX 2% xylose	0.273	< 0.01	0.041	0.148	0.197 ± 0.006	This study
		Anaerobic batch, YNBX 2% xylose	0.323	< 0.01	0.044	0.131	0.052 ± 0.006	This study
H132-A^{SB}	Selection of H132-A, aerobic sequential batch	Anaerobic batch, YNBX 2% xylose	0.357	< 0.01	0.032	0.090	0.050 ± 0.009	This study
H131-A3^{SB-2}	Selection of H131-A3, micro-aerobic sequential batch	Anaerobic batch, 2 × YNB 4% xylose	0.421	< 0.01	0.111	0.262	0.061 ± 0.001	This study
H131-A3^{SB-3}	Selection of H131-A3, anaerobic sequential batch	Anaerobic batch, 2 × YNB 4% xylose	0.427	< 0.01	0.277	0.649	0.073 ± 0.002	This study
H131-A3^{CS}	Selection of H131-A3, anaerobic chemostat	Anaerobic batch, 2 × YNB 4% xylose	0.425	< 0.01	0.399	0.939	0.120 ± 0.004	This study
		Anaerobic chemostat, YNBX	0.438	< 0.01	0.687	1.568	0.148[b]	This study
H131-A3-AL^{CS}	H131-A3^{CS}, *ARG4 LEU2*	Anaerobic batch, 2 × YNB, 4% xylose, ergosterol and Tween 80	0.410	< 0.01	0.765	1.866	0.203 ± 0.006	This study
RWB 217	*XYLA*, *XKS1*, *TAL1*, *TKL1*, *RPE1*, *RKI1*, *gre3Δ*	Anaerobic batch, synthetic medium	0.43	0.003	0.46	1.06	0.09	Kuyper et al. (2005a)
RWB 218	Selection of RWB 217	Anaerobic batch, synthetic medium	0.41	0.001	0.49	1.2	0.12	Kuyper et al. (2005b) and van Maris et al. (2006)

[a] Average specific ethanol production and xylose consumption rates calculated from entire fermentation of aerobic batch and growth phase of anaerobic batch.
[b] Maximum dilution rate in chemostat, equivalent to maximum specific growth rate.

was used to initiate the evolution process, which consisted of three stages.

The first stage of evolution was carried out through sequential batch cultivation under aerobic conditions in SDX medium. Once the culture reached the stationary phase, it was re-inoculated to a new batch at dry cell weight of about 0.015 g DCW/L. After about 70 generations of evolution, a single strain, H131-A3^{SB-1} (Table 2), was isolated, which showed an improved aerobic growth.

The entire population from which H131-A3^{SB-1} was isolated was further evolved, first micro-aerobically and later anaerobically using the same sequential batch cultivation setup, except that YNBX medium was used instead of SDX medium. For micro-aerobic cultivation, the flasks were plugged to avoid oxygen diffusion, while anaerobic conditions were achieved by sparging nitrogen at the beginning of and during sampling. After about 60 generations of micro-aerobic selection, a single strain with the best anaerobic specific growth rate was isolated and named H131-A3^{SB-2} (Table 2). The sequential batch cultivation was then switched to anaerobic conditions for another 60 generations of evolution. Strain H131-A3^{SB-3} (Table 2) was then isolated using a similar approach.

At the third stage, the evolution process subjected the entire population from which strain H131-A3^{SB-3} was selected to anaerobic continuous cultivation using xylose as the limiting carbon source. Chemostat cultivation was initiated using stationary phase cells in the bioreactor with an initial dilution rate of 0.02 h^{-1} and feeding YNBX. The dilution rate was increased stepwise once the culture reached steady state, which is defined by a stable cell density for 48 h or 3 retention times, whichever came first. After approximately 60 generations, the dilution rate had been increased from 0.02 to 0.12 h^{-1} with the cell density of about 0.6 g DCW/L. In order to further increase xylose selective pressure and improve xylose uptake at a lower titer, the feed xylose concentration was reduced from 20 g/L to 10 g/L for another 40 generations. In the end, a steady state was achieved with cell density of 0.56 g DCW/L and a dilution rate of 0.148 h^{-1}. Xylose consumption rate was 1.464 $g\,g^{-1}\,h^{-1}$ with ethanol yield of 0.438 $g\,g^{-1}$ xylose (Table 4). A single strain was then isolated and named H131-A3^{CS} (Table 2) for further characterization.

The various evolved strains were characterized with respect to their growth and fermentation rates in various media: H131-A3^{SB-1} was characterized in aerobic batch cultivation in shake flasks with SDX medium, and also in anaerobic batch cultivation in shake flasks with YNBX medium; H131-A3^{SB-2}, H131-A3^{SB-3} and H131-A3^{CS} were evaluated under anaerobic conditions on 2 × YNBX medium with 4% of xylose. Initial growth OD measurements were used to determine the μ_{max} of each strain on xylose. Additionally, growth phase metabolites measurement allowed determination of the rates of xylose consumption and ethanol production, as well as the xylose/ethanol conversion yield.

The anaerobic growth, xylose consumption and ethanol production rates of the various strains displayed remarkable improvement along the evolution path. H131-A3^{SB-1} showed improved aerobic growth and xylose consumption (Table 4), albeit with low ethanol

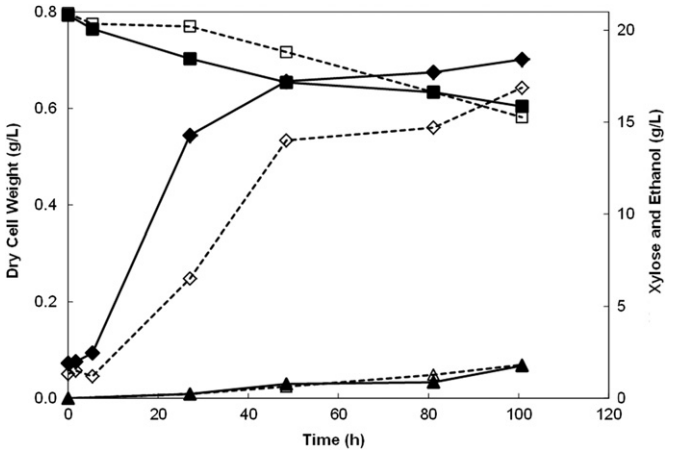

Fig. 1. Anaerobic fermentation of evolved *S. cerevisiae* strain H131-A3^{SB-1} and H132-A^{SB} on YNBX medium with 20 g/L xylose. H131-A3^{SB-1}: ♦, dry cell weight (g/L); ■, residual xylose (g/L); ▲, ethanol production (g/L). H132-A^{SB}: ⋄, dry cell weight (g/L); □, residual xylose (g/L); △, ethanol production (g/L).

yield and anaerobic growth rate (Fig. 1 and Table 4). The micro-aerobically evolved H131-A3^{SB-2} showed slightly improved anaerobic growth and a xylose consumption rate about two times that of H131-A3^{SB-1} (Fig. 2 and Table 4). The further evolved H131-A3^{SB-3} and H131-A3^{CS} displayed about 20% and 100% faster anaerobic growth than that of H131-A3^{SB-2} (Fig. 2 and Table 4). The xylose consumption rates of strains H131-A3^{SB-3} and H131-A3^{CS} were about four and six times that of the H131-A3^{SB-1}. Put differently, while it took about 80 h for H131-A3^{CS} to deplete the xylose, H131-A3^{SB-3} required 120 h and xylose was not used after 120 h of fermentation with H131-A3^{SB-2}. It took progressively longer time to consume the remaining 10 g/L of xylose for less evolved strains (H131-A3^{CS}, H131-A3^{SB-3} and H131-A3^{SB-2}). This is reflected in the estimated specific xylose consumption rates which, at a xylose concentration of 10 g/L, are 35% and 20% higher for strain H131-A3^{CS} than those of strains H131-A3^{SB-2} and H131-A3^{SB-3}, respectively. Under anaerobic conditions, the three strains had very close final biomass concentrations (~1.5 g/L DCW), ethanol yield (0.42 g/g xylose), glycerol yield (~0.04 g/g xylose) and low xylitol yield (~0.005 g/g xylose, the quantification was approximate since xylitol accumulation was at the detection limit of the HPLC).

3.3. Complementation of arg4 and leu2

The evolutionarily engineered strain H131-A3^{CS} still contained two auxotrophic markers, *arg4* and *leu2*, requiring supplementation of L-arginine and L-leucine in the medium. To eliminate the need for L-arginine and L-leucine, the *arg4* and *leu2* were complemented by pUCAR1 and YIp pRS405 (Table 1), separately. H131-A3^{CS} was first transformed with *Cla* I linearized pUCAR1 (Table 1) and selected on Arg$^-$ medium to yield H145E8-A3 (Table 2). H145E8-A3 was further transformed with *Afl* II digested pRS405 and selected on Leu$^-$ medium to yield H131-A3-AL^{CS} (Table 2). The aerobic growth of the new constructed H131-A3-AL^{CS} was greatly improved compared with the parent strain H131-A3^{CS} on minimum medium (data not shown). However, the anaerobic growth of H131-A3-AL^{CS} was similar to that of H131-A3^{CS} (data not shown), implying that the growth of H131-A3-AL^{CS} was otherwise limited under anaerobic condition. Therefore, the medium was supplemented with the anaerobic growth factors ergosterol and Tween 80. As shown in Fig. 2, H131-A3-AL^{CS} showed unprecedented anaerobic growth rate of $0.203 \pm 0.006\ h^{-1}$ and a xylose consumption rate of $1.866\ g\ g^{-1}\ h^{-1}$, 14 times as high as that of H131-A3^{SB-1}.

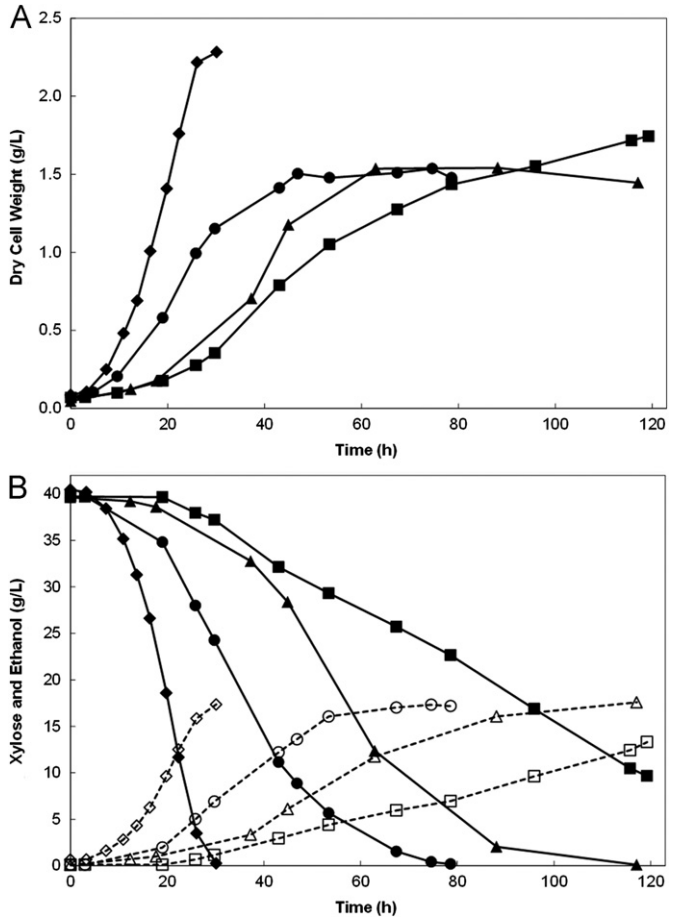

Fig. 2. Anaerobic fermentation of evolved *S. cerevisiae* strains (H131-A3^{SB-2}, H131-A3^{SB-3}, H131-A3^{CS} and H131-A3-AL^{CS}) on YNBX medium with 40 g/L xylose. 0.01 g/L ergosterol and 0.42 g/L Tween 80 supplemented for fermentation of H131-A3-AL^{CS}. (A) Dry cell weight (g/L): ■, H131-A3^{SB-2}; ▲, H131-A3^{SB-3}; ●, H131-A3^{CS}; ♦, H131-A3-AL^{CS}. Initial cell density was 0.05 g DCW/L. (B) Residual xylose (g/L): ■, H131-A3^{SB-2}; ▲, H131-A3^{SB-3}; ●, H131-A3^{CS}; ♦, H131-A3-AL^{CS}. Ethanol production (g/L): □, H131-A3^{SB-2}; △, H131-A3^{SB-3}; ○, H131-A3^{CS}; ⋄, H131-A3-AL^{CS}.

3.4. Inverse metabolic engineering identifies XYLA multi-copy inserts as a key component of evolved strains

While evolutionary engineering is very effective in generating strains with drastically improved production phenotypes, it provides no information on the genotypic changes underlying such improvements. To identify some of the genetic factors responsible for the improved xylose assimilation phenotype of the evolved strains, we deployed Inverse Metabolic Engineering whereby the unevolved *S. cerevisiae* strain H131-A3 was complemented with genomic DNA fragments of the evolved strain H131-A3^{SB-3}. Construction of *S. cerevisiae* H131-A3^{SB-3} genomic library yielded an *E. coli* library of 5×10^5 CFU on plates. Based on colony counting after serial dilution and re-plating on an X-Gal plate, about 90% of the colonies contained inserts. The quality of the library was also assessed by plasmid digestion, which showed an average insert size of 3–5 kbps (data not shown). The library was then transformed to H131-A3 and plated on SD medium containing 20 g/L glucose, to yield about 3×10^5 yeast colonies.

A high-throughput micro-fluidic screening system (Wang, 2009; Wang et al., 2008) was used to screen the yeast library H131-A3 (pRS415-geno) for high xylose consuming strains. The method measures xylose consumption of each single cell, individually encapsulated in separate water droplets of 40–70 μm diameter

dispersed in oil medium. Xylose concentration was assayed in each droplet and those with low xylose concentration (indicating high xylose consumption rate) were sorted for further analysis (The mechanism of the micro-fluidic platform is shown in the supplementary material, more details of this research conducted by Benjamin L. Wang et al. are reported separately). The strains selected through the micro-fluidic device screening were grown on SDX medium to confirm the improvement of growth and xylose-assimilation phenotypes. So verified strains were further validated by isolation and retransformation of the pRS415-geno plasmids to H131-A3.

Four isolates were obtained, from which plasmids were prepared for insert identification by DNA sequencing and restriction enzyme digestion. Interestingly, all four plasmids displayed highly similar structures. Here (Fig. 3), we show the results of the analysis of one plasmid (pRS415-geno-W2) isolated from the strain identified with the micro-fluidic screening platform to demonstrate the sequence structure.

DNA sequencing using primers complementary to the plasmid backbone and the *XYLA* gene showed that plasmid pRS415-geno-W2 contained at least one full ORF of *XYLA* gene plus two truncated fragments of the ORF (Fig. 3A). The plasmid pRS415-geno-W2 was digested by the restriction enzyme *Kpn* I to obtain further details of the plasmid sequence. It was confirmed that the *XYLA* gene construct (*TDH3p-XYLA-CYC1t*, 2.2 kbps) was indeed present on the plasmid (Lane 1 from Fig. 3B) at more than one copy, as indicated by the intensity of the 2.2 kbps band which was even higher than that of the 5319 bps band. As a control, digestion analysis for the plasmid pRS415 was also performed using the same restriction enzymes (Fig. 3B, Lanes 2 and 4). To determine the *XYLA* gene copy number on pRS415-geno-W2, an *EcoR* I digest was performed to confirm that the size of the plasmid was about 14 kbps (Lane 3 from Fig. 3B). We thus determined that there were three full copies of the *TDH3p-XYLA-CYC1t* construct by comparing Lane 1 and Lane 3 from Fig. 3B [$(\sim 10{,}000+3962) - (5319+1621+688)\ \text{bps} \approx 3 \times 2.2$ kbps]. The copy number was also verified by analyzing the band intensity of Lane 1 from Fig. 3B. It was concluded that the insert carried by pRS415-geno-W2 has three full *XYLA* gene constructs with truncated constructs flanking on each side (Fig. 3C).

Other isolated plasmids contain similar tandem duplication of *XYLA*, but vary in copy number, digestion site and orientation of

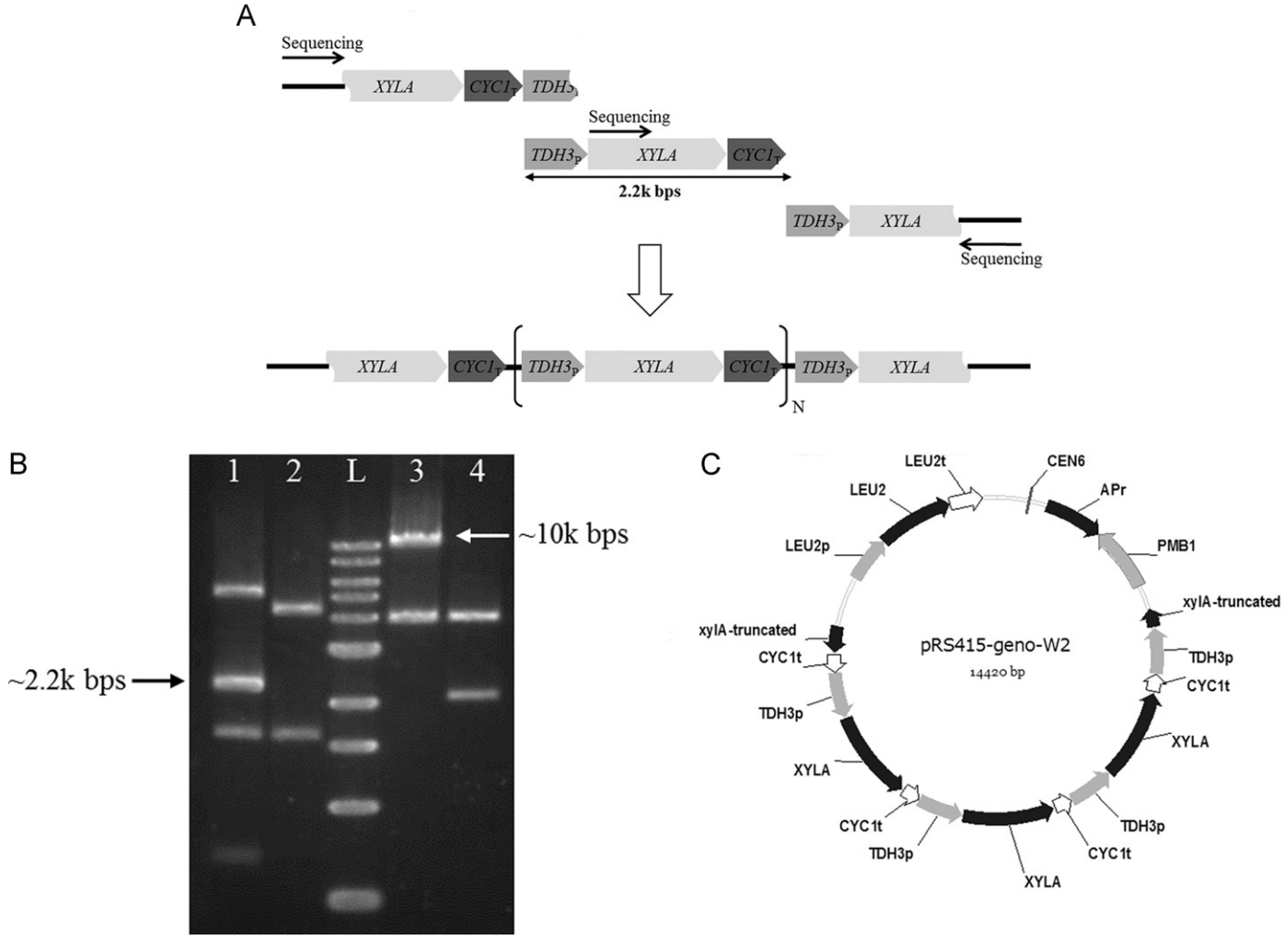

Fig. 3. Sequencing and restriction enzyme digest analysis of pRS415-W2. pRS415-geno-W2 carries three full *XYLA* gene constructs with truncated constructs flanking on each side. (A) Sequencing results of plasmid pRS415-geno-W2. Sequencing from both end of the insert and the beginning of the *XYLA* ORF revealed duplication of *XYLA* expression structure. (B) Restriction enzymes digestion of plasmid pRS415-geno-W2 and control pRS415. Lane 1: pRS415-geno-W2 digested with *Kpn* I (5319 bps, 2264 bps, 1621 bps, 688 bps); Lane 2: pRS415 digested with *Kpn* I (4400 bps, 1621 bps); Lane L: DNA ladder (10 kbps, 8 kbps, 6 kbps, 5 kbps, 4 kbps, 3 kbps, 2 kbps, 1.5 kbps, 1 kbps, 0.5 kbps); Lane 3: pRS415-geno-W2 digested with *EcoR* I (10458 bps, 3962 bps); Lanes 4: pRS415 digested with *EcoR* I (3962 bps, 2059 bps). (C) Map of plasmid pRS415-geno-W2.

insert. The above observations imply that an increased copy number of *XYLA* contributes to the improved xylose utilization in the evolved strains.

3.5. Evolved strains exhibiting high xylose assimilation rates harbor a large number of XYLA copies with similar high enzymatic activity

The copy numbers of genes *XYLA* and *XYL3* in the unevolved H131-A3 and the evolved H131-A3^{SB-3}/H131-A3^{CS} strains were determined through quantitative PCR. The copy numbers of *XYLA* and *XYL3* per genome were calculated by comparing their relative amount to the *PGK1* gene present in the same sample, assuming a single copy of *PGK1* per haploid genome. *PGK1* gene encoding 3-phosphoglycerate kinase, a key enzyme in glycolysis and gluconeogenesis, is a highly-expressed gene and its mRNA is relatively stable. Obtained molecular and biochemical characterizations of *XYLA* and *XYL3* (normalized to reference strain H131-A3) are summarized in Fig. 4. The gene copy numbers of *XYLA* and its expression level for both evolved strains were found to be 8–32 times higher than that of the reference strain, with a good correlation among DNA, RNA and protein activity. For *XYL3* the DNA, RNA, and protein levels of the evolved strains were comparable to the reference strain with good correlation (a system error of about twofold).

In order to confirm that a high *XYLA* copy number can increase substantially the xylose assimilation rate, a new xylose metabolizing strain was constructed based on H131, with one copy of *PsXYL3* integrated in the genome to achieve moderate activity of xylulokinase. The *TDH3* promoter that driving *XYL3* gene was replaced by the constitutive truncated *HXT7* promoter (Hauf et al., 2000) to avoid further recombination with *TDH3p-XYLA*. The *HXT7p-PsXYL3-CYC1t* construct was then cloned into pUCAR1-*PsXYL3* and transformed to H131, resulting in H132 (Table 2). H132 was transformed with integration plasmid pRS406-$(XYLA)_2$, which carries two tandem copies of the *XYLA* construct and integrated into the *ura3* locus on chromosome V of H132. The resulting strain H132-A was then evolved in an aerobic sequential batch cultivation process with SDX medium for about 30 generations, similar to the evolution of H131-A3. The fermentation performance of the resulting strain, H132-A^{SB} (Table 2), is comparable to that of strain H131-A3^{SB-1}, as shown in Fig. 1 and Table 4. Copy number measurement with quantitative PCR revealed 31.59 ± 3.45 copies of *XYLA* in H132-A^{SB}, significantly higher than the 2.44 ± 0.89 (theoretical copy number is 2) initial copies of the unevolved H132-A strain. Quantitative RT-PCR showed a 19-fold increase in *XYLA* transcription in H132-A^{SB} from the levels of H132-A.

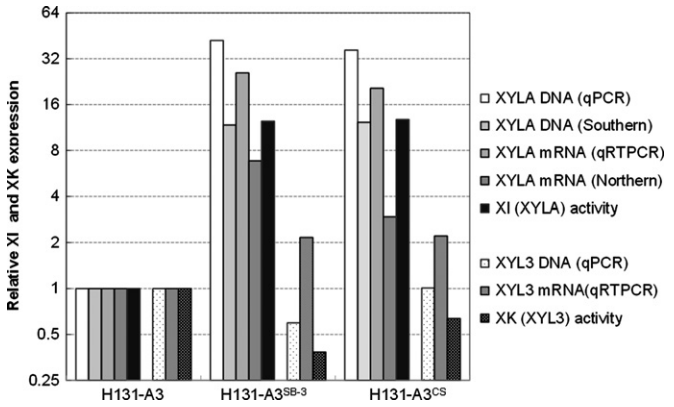

Fig. 4. Copy number, transcription level and activity of *XYLA* and *XYL3*. All values are plotted with reference to H131-A3. For absolute value of the measurements: *XYLA* copy#, 1.20 ± 0.22; *XYL3* copy#, 1.53 ± 0.68 copies; XI activity, 0.044 ± 0.002 U/mg; XK activity, 1.414 ± 0.072 U/mg.

The location of *XYLA* in the evolved strains was confirmed through PFGE followed by chromosome blotting. In the evolved H131-A3^{SB-3}, the *XYLA* duplication structure was determined to be on the chromosome VI (Fig. 5). The integration also changed the size of chromosome VI from 270 kbps to about 380 kbps, which is consistent with the copy number measurement results (2.2 kbps/copy $\times$ 47 copies $\approx$ 103 kbps). For the other evolutionarily engineered strain H132-A^{SB}, the *XYLA* duplication structure was detected to be in the *URA3* locus of chromosome V as expected, which was confirmed by using PCR with primers on the chromosome side before *URA3* and on the plasmid side in *XYLA*. The chromosome V size migration was about 70 kbps (577 kbps to $\sim$650 kbps), in agreement with the copy number determined by qPCR (2.2 kbps/copy $\times$ 32 copies $\approx$ 70 kbps).

3.6. Evolution and carbon source change elicit significant transcriptional reprogramming

Global transcriptional analysis was carried out to evaluate the effect of evolution and carbon source on gene expression levels under three different strain/culture conditions: BF264-15D on glucose (Un/G: Unevolved/Glucose), H131-A3^{CS} on glucose (Ev/G: Evolved/Glucose) and H131-A3^{CS} on xylose (Ev/X: Evolved/Xylose). Both the evolution and the carbon source significantly affect genes expression in anaerobic fermentation. Of the 6799 probes detected under the three different culture conditions, 748

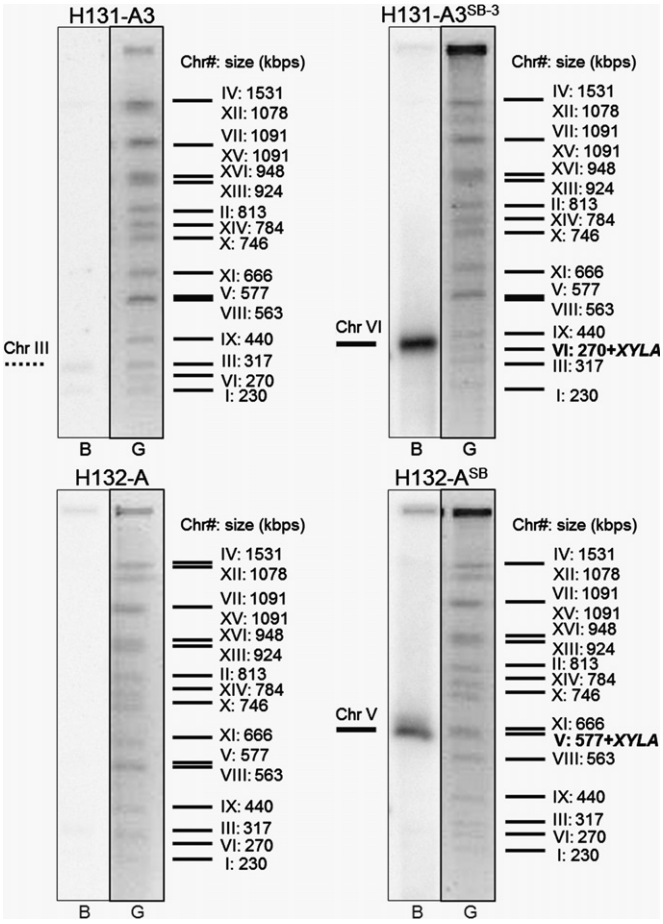

Fig. 5. Chromosome location of the *XYLA* duplication. G: Gel, PFGE (color-inverted) of the chromosomes from the evolved strains and the reference strain, chromosome number and size are labeled in the right. B: Blot, hybridization of the corresponding chromosome blot with the *XYLA* probe; in strain H131-A3^{SB-3}, the *XYLA* duplication structure is on the Chr VI; in strain H132-A^{SB}, the *XYLA* duplication structure is in the *URA3* locus of the Chr V.

Table 5
Overrepresented pathways of differentially expressed genes in each cluster.

Set	Enriched pathway	Number of genes	*p*-Value
Up-regulated			
Cluster_1	Cell cycle – yeast	5	0.006
Cluster_2	Galactose metabolism	2	0.034
Cluster_2	Pyrimidine metabolism	4	0.025
Cluster_2	Ribosome	6	0.021
Cluster_2	Cell cycle – yeast	5	0.044
Cluster_2	Phenylalanine metabolism	2	0.01
Cluster_4	Ribosome	4	1.16E−04
Cluster_5	Ribosome	10	2.61E−09
Cluster_5	Metabolic pathways	8	0.018
Cluster_5	Cysteine and methionine metabolism	2	0.012
Cluster_5	Tyrosine metabolism	2	0.005
Cluster_5	Pentose phosphate pathway	3	5.35E−04
Cluster_6	Ribosome	15	1.28E−12
Down-regulated			
Cluster_5	Histidine metabolism	2	0.004
Cluster_5	Citrate cycle (TCA cycle)	2	0.023
Cluster_5	Metabolic pathways	14	4.71E−05
Cluster_5	Cysteine and methionine metabolism	2	0.018
Cluster_5	Glycolysis/gluconeogenesis	2	0.039
Cluster_5	Alanine, aspartate and glutamate metabolism	3	8.17E−04
Cluster_5	Valine, leucine and isoleucine degradation	2	0.001
Cluster_8	Metabolic pathways	8	0.037
Cluster_10	Starch and sucrose metabolism	2	0.027

(11%) were differentially expressed when comparing Un/G and Ev/G, and 519 genes (7.6%) showed differential expression for growth of the evolved strain H131-A3^{CS} on glucose and xylose. Taking into account both the evolution and carbon source change, 775 genes (11.4%) showed differential expression, with 433 (6.4%) up-regulated and 342 (5%) down-regulated. The 775 genes whose mRNA levels changed significantly between Un/G and Ev/X were analyzed for pathway enrichment, as shown in Table 5. Genes involved in ribosome, amino acid metabolism, cell cycle and energy production changed the most. Relative mRNA levels (data from microarray and qPCR) of genes responsible for the energy production are summarized in Fig. 6.

mRNA levels of *XYLA* changed significantly after evolution, confirming the findings of previous sections. *PsXYL3* and endogenous *XKS1* exhibited relatively moderate expression over the three culture conditions. The non-oxidative pentose phosphate pathway (*RKI1*, *RPE1* and *TKL1*) was much up-regulated due to the overexpression of those genes. *PsTAL1* showed similar expression level as the other three PPP genes, although down-regulated over the evolution. Transcripts for the gluconeogenic enzymes, encoded by *PCK1*, *FBP1* and *ICL1*, were induced 8.3-, 2.2-, and 2.1-fold by xylose, respectively. For the fermentation pathway, expression of *ADH1* and *ADH2* were induced 2.4- and 2.1-fold, respectively. In addition, *ALD3* was down-regulated by 4.5-fold, favoring the formation of ethanol over acetate. Transcript levels of most other genes did not change significantly when comparing Un/G and Ev/X.

4. Discussion

We have applied evolutionary engineering to a metabolically engineered *S. cerevisiae* strain to improve growth and fermentation on xylose. Both the anaerobic growth rate and the xylose consumption rate were significantly elevated in the ultimately evolved strain H131-A3-AL^{CS}. Ethanol yields remained close to the theoretical maximum in most strains.

Evolved strains exhibiting high xylose assimilation rates harbor a large number of *XYLA* copies, which is consistent with the high transcription level of *XYLA* and high enzymatic activity of XI. The genotype of *XYLA* integration and duplication was further verified by construction of another xylose-utilizing strain, H132-A^{SB}, in a similar way. We hypothesize that the high copy number of *XYLA* is necessary for xylose assimilation, and the duplication initiated through the unequal crossover of the *TDH3p-XYLA-CYC1t – TDH3p-PsXYL3-CYC1t* construct on the plasmid pRS426-*XYLA-XYL3*, and elongated thereafter (Fig. 7). One piece of evidence supporting this hypothesis is that the *Kpn* I site among *XYLA* duplication after evolution was from the original pRS426-*XYLA-XYL3*, between the *XYLA* and *XYL3*. Moreover, recombination could occur more frequently than cell mitosis, since pRS426-*XYLA-XYL3* is a multiple-copy plasmid. Nevertheless, repeated attempts at isolating the recombined plasmid pRS426-$(XYLA)_N$-*XYL3* from evolved H131-A3 strains were unsuccessful. Further effort to cure the pRS426 plasmid from the evolved H131-A3 strains based on the *URA3*/5-FOA counter-selection resulted in a strain with *ura3* genotype, but retained xylose-utilizing ability. All these observations suggested that *XYLA* had recombined onto the genome after evolutionary engineering. Although the *XYLA* duplication structure was not verified at the molecular level, the chromosome blot, qPCR results and tandem gene duplication structure on pRS415-geno-W2 strongly suggest that duplication and integration of gene *XYLA* was the major recombination event during evolutionary engineering. High expression level of heterologous XI promotes rapid xylose utilization.

Inverse metabolic engineering based on functional complementation is a useful approach to identify dominant genotypes of the evolutionary engineered strains. This requires good coverage of the genomic library and a screening method with high efficiency. In the present work, proper library sizes in both *E. coli* and yeast (10^5–10^6) could be obtained. In general, conventional screening methods based on growth rate and colony formation can work effectively for the screening of the genomic library and identification of substrate utilization related genes (Jin et al., 2005; Ni et al., 2007). However, "good" transformants in the genomic library of the present work displayed only minor growth advantage, and colony-size-based screening could hardly identify any fast xylose-utilizing clones from the genomic library. This problem was solved with the use of the micro-fluidic screening system that assesses the metabolic activity of single cells encapsuled in droplets and sorts cells according to their individual xylose consumption rate. Plasmid pRS415-geno-and other isolated plasmids all contained multiple copies of *XYLA* expression construct plus two truncated copies flanking in each side. The size of the insert ranged from 8.4 to 10.6 kbps, and exceeded the size of DNA collected from the gel (up to 8 kbps) for the ligation. Therefore, it is likely that recombination of *XYLA* constructs occurred during the pre-culture before the micro-fluidic screening, resulting in an increased copy number of *XYLA* on the plasmid. To avoid extensive sub-cultivation before the screening, the screening needed to be fine-tuned to achieve better throughput and resolution.

Transcriptional results showed that evolution and carbon source can cause significant changes in gene expression. Genes involved in energy production, the xylose metabolic pathway and the pentose phosphate pathway were overexpressed to support rapid xylose assimilation. The fermentation pathway (*ADH1,2* and *ALD3*) was also reprogrammed to facilitate ethanol formation. Transcripts for the gluconeogenic enzymes (*PCK1*, *FBP1* and *ICL1*) were greatly induced by xylose, consistent with other literature reports (Jin et al., 2004; Wahlbom et al., 2003). Ribosome and amino acid metabolism also significantly changed during evolution on xylose, possibly due to the overexpression of the xylose

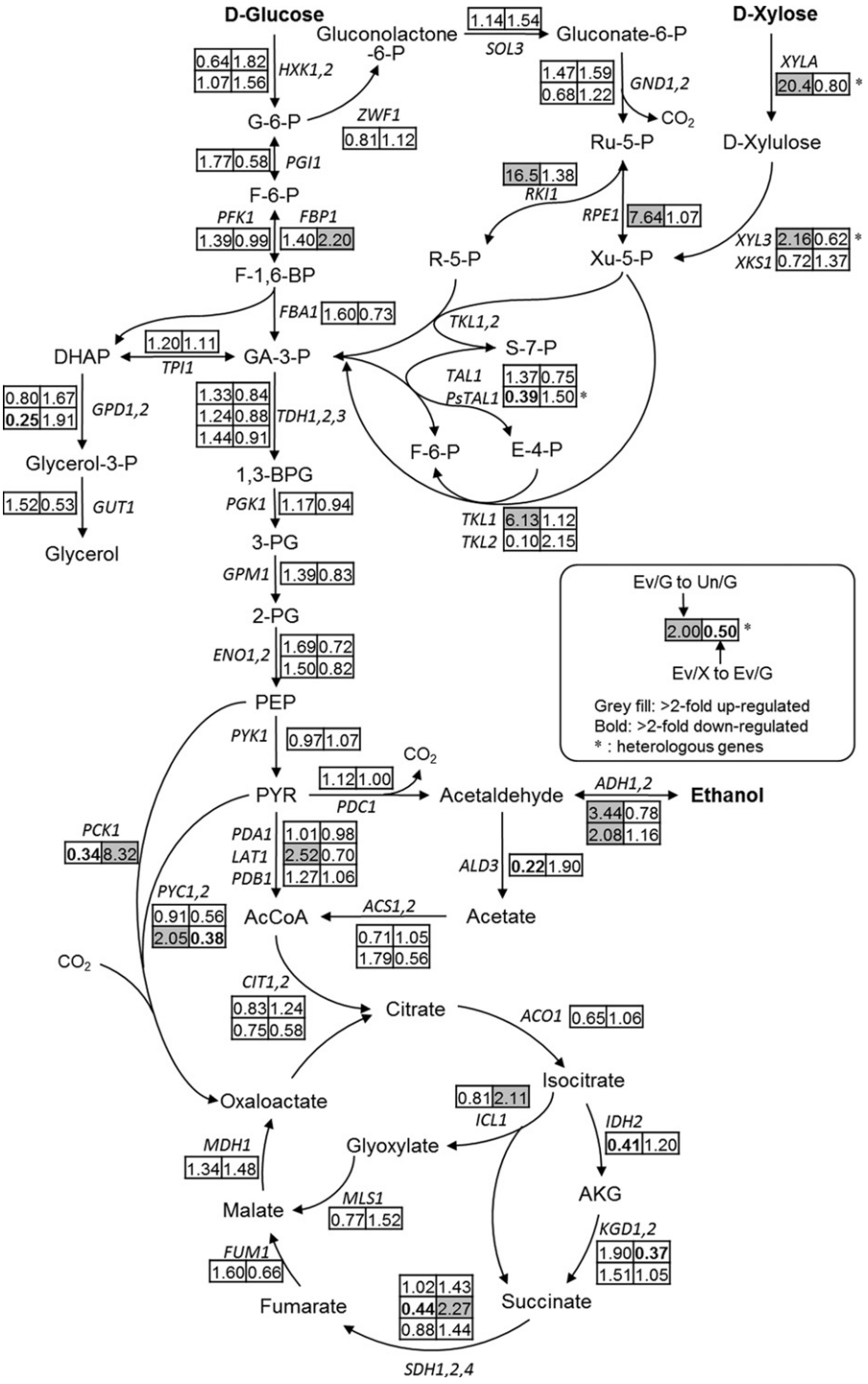

Fig. 6. Relative mRNA levels of genes responsible for energy production during glucose and xylose metabolism under anaerobic conditions. The numbers inside each box indicate the ratio of transcripts for strains grown on xylose and glucose. Results of evolved H131-A3^{CS} compared with the wild type BF264-15Dau (H131 for heterologous genes) on glucose are shown on the left side of each pair of boxes. Results of evolved H131-A3^{CS} on xylose compared with on glucose are shown on the right side of each pair of boxes. Transcript levels that increased more than twofold are shown in gray fill. Transcript levels that decreased more than twofold are shown in bold font. The nomenclature follows that of the Saccharomyces Genome Database (http://www.yeastgenome.org/).

metabolic pathway and pentose phosphate pathway. It will be of interest to measure the time course of gene expression during the evolution process in order to identify the key mutational events that contributed to the new phenotypes.

The successful restoration of the *ARG4* and *LEU2* genes eliminated the requirement of arginine and leucine supplementation in the medium. Moreover, restoration of *LEU2* increased the anaerobic growth rate by 30% (data not shown). It has been reported that the amount of leucine provided in commonly used synthetic media (YNB with 100 mg/L leucine in this study) is limiting for the growth of leucine-requiring strains, leading to the recommendation to supplement synthetic media with a higher leucine concentration (Pronk, 2002). Further experiments showed that 200–400 mg/L of leucine could largely restore the growth deficiency of the *leu2*-strain (data not shown), consistent with Pronk's observation. In addition, studies have demonstrated that leucine

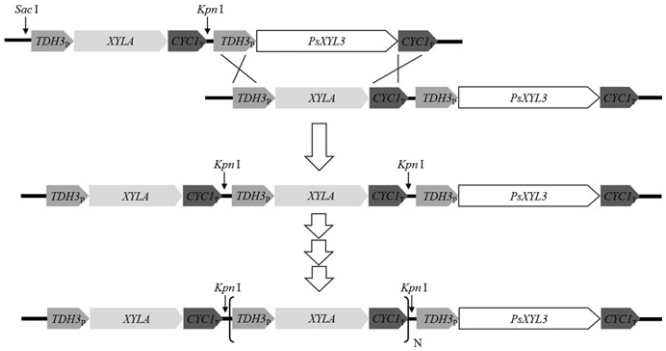

Fig. 7. Scheme of unequal crossover of pRS426-*XYLA*-*XYL3* and duplication of *XYLA* × indicates homologous recombination between *TDH3* promoter regions and *CYC1* terminator regions of two plasmids.

correlates with tolerance to ethanol (Baerends et al., 2009). Therefore, a functional leucine pathway is preferable to leucine supplementation while engineering strains for better growth and productivity.

Ergosterol and Tween 80 are important anaerobic growth factors (Andreasen and Stier, 1953, 1954; Ohta and Hayashida, 1983), and are routinely used under strictly anaerobic conditions. With the supplementation of ergosterol and Tween 80, strain H131-A3^{CS} improved dramatically its anaerobic growth rate ($\mu_{max}=0.203\pm0.006\ h^{-1}$) and specific xylose consumption rate ($1.866\ g\ g^{-1}\ h^{-1}$,Table 4), which are 70% and 50%, respectively, higher than those of the best reported strain RWB 218 (Kuyper et al., 2005b; van Maris et al., 2006). This makes the fermentation performance of strain H131-A3-AL^{CS} superior to any other strain reported to-date.

The three stages of the strain evolution path were designed such as to sequentially improve first the biomass yield, then the anaerobic fermentation and finally the anaerobic growth rate, all on xylose. A relatively rich medium (SDX) was used for the aerobic stage of evolution to promote cell growth. At the end of the stage, the biomass yield was as high as 0.5 g DCW/g xylose with low to moderate xylose consumption rate and marginal fermentation rate. As such, the xylose metabolic pathway was validated and growth on xylose was established. For the second stage of oxygen limited sequential batch cultivation, it was hypothesized that alcoholic fermentation would be the major pathway of xylose utilization under the oxygen-limited conditions, and cell growth would be highly correlated with xylose consumption. As a result, the major phenotypic difference observed between strains H131-A3^{SB-2} and H131-A3^{SB-3} is the elevated xylose consumption rate of the latter. The third stage of evolution in a continuous flow chemostat was conducted at a relatively low cell density (about 0.5 g DCW/L), similar to the exponential growth phase in batch cultivation. As expected, remarkable improvement was achieved in the specific growth rate ($0.120\ h^{-1}$ for strain H131-A3^{CS} versus $0.073\ h^{-1}$ for H131-A3^{SB-3}). The high dependence of the growth rate on the substrate uptake rate increased the effectiveness of the chemostat evolution as the population was continuously propagated under the selective pressure of xylose as a substrate. Thus, initial adaptation followed by chemostat cultivation under proper substrate pressure can be an effective strategy of evolutionary engineering to improve the substrate uptake.

Xylose transport was also possibly improved during evolution. However, sequencing of the major monosaccharide transporters in the evolved strains did not reveal any mutations. Therefore, the improvement of xylose transport is probably due to the changes in the transporter expression rather than the transporter protein evolution.

In summary, combining metabolic with evolutionary engineering gave rise to new strains of *S. cerevisiae* with greatly improved anaerobic growth rate, xylose consumption rate and ethanol production. Further optimization resulted in the strain H131-A3-AL^{CS} which exhibited the performance superior to any other reported strain. Genetic analysis on the evolved strain identified high copy number of xylose isomerase, through *XYLA* duplication and genomic integration, as the major recombination event during the evolution. This was further verified by showing that strains with very high *XYLA* copy number have very high xylose assimilation rates.

Acknowledgments

This project was financially supported by the MIT Energy Initiative and the Low Carbon Emissions University Alliance (LCEUA). We thank Paula Grisafi, Anna Drinnenberg for sharing the expertise on PFGE and chromosome blot.

Appendix A. Supporting information

Supplementary data associated with this article can be found in the online version at http://dx.doi.org/10.1016/j.ymben.2012.07.011.

References

Akinterinwa, O., Cirino, P.C., 2009. Heterologous expression of D-xylulokinase from *Pichia stipitis* enables high levels of xylitol production by engineered *Escherichia coli* growing on xylose. Metab. Eng. 11, 48–55.

Amore, R., Wilhelm, M., Hollenberg, C.P., 1989. The fermentation of xylose—an analysis of the expression of bacillus and actinoplanes xylose isomerase genes in yeast. Appl. Environ. Microbiol. 30, 351–357.

Andreasen, A.A., Stier, T.J., 1953. Anaerobic nutrition of *Saccharomyces cerevisiae*. I. Ergosterol requirement for growth in a defined medium. J. Cell. Physiol. 41, 23–36.

Andreasen, A.A., Stier, T.J., 1954. Anaerobic nutrition of *Saccharomyces cerevisiae*. II. Unsaturated fatty acid requirement for growth in a defined medium. J. Cell. Physiol. 43, 271–281.

Baerends, R.J., Qiu, J.L., Rasmussen, S., Nielsen, H.B., Brandt, A., 2009. Impaired uptake and/or utilization of leucine by *Saccharomyces cerevisiae* is suppressed by the SPT15-300 allele of the TATA-binding protein gene. Appl. Environ. Microbiol. 75, 6055–6061.

Becker, J., Boles, E., 2003. A modified *Saccharomyces cerevisiae* strain that consumes L-arabinose and produces ethanol. Appl. Environ. Microbiol. 69, 4144–4150.

Bieche, I., Olivi, M., Champeme, M.H., Vidaud, D., Lidereau, R., Vidaud, M., 1998. Novel approach to quantitative polymerase chain reaction using real-time detection: application to the detection of gene amplification in breast cancer. Int. J. Cancer 78, 661–666.

Brat, D., Boles, E., Wiedemann, B., 2009. Functional expression of a bacterial xylose isomerase in *Saccharomyces cerevisiae*. Appl. Environ. Microbiol. 75, 2304–2311.

Bruinenberg, P.M., Debot, P.H.M., Vandijken, J.P., Scheffers, W.A., 1983. The role of redox balances in the anaerobic fermentation of xylose by yeasts. Eur. J. Appl. Microbiol. Biotechnol. 18, 287–292.

Carle, G.F., Olson, M.V., 1985. An electrophoretic karyotype for yeast. Proc. Natl. Acad. Sci. U.S.A. 82, 3756–3760.

Gardonyi, M., Hahn-Hägerdal, B., 2003. The Streptomyces rubiginosus xylose isomerase is misfolded when expressed in *Saccharomyces cerevisiae*. Enzyme Microb. Technol. 32, 252–259.

Hahn-Hägerdal, B., Karhumaa, K., Jeppsson, M., Gorwa-Grauslund, M.F., 2007. Metabolic engineering for pentose utilization in *Saccharomyces cerevisiae*. Adv. Biochem. Eng. Biotechnol. 108, 147–177.

Hauf, J., Zimmermann, F.K., Muller, S., 2000. Simultaneous genomic overexpression of seven glycolytic enzymes in the yeast *Saccharomyces cerevisiae*. Enzyme Microb. Technol. 26, 688–698.

Ho, N.W., Chen, Z., Brainard, a. P., 1998. Genetically engineered Saccharomyces yeast capable of effective cofermentation of glucose and xylose. Appl. Environ. Microbiol. 64, 1852-1859.

Jeffries, T.W., 1983. Utilization of xylose by bacteria, yeasts, and fungi. Adv. Biochem. Eng. Biotechnol. 27, 1–32.

Jin, Y.-s., Laplaza, J.M., Jeffries, T.W., 2004. *Saccharomyces cerevisiae* engineered for xylose metabolism exhibits a respiratory response. Appl. Environ. Microbiol. 70, 6816–6825.

Jin, Y.-s., Ni, H., Laplaza, J.M., Jeffries, T.W., 2003. Optimal growth and ethanol production from xylose by recombinant *Saccharomyces cerevisiae* require moderate D-xylulokinase activity. Appl. Environ. Microbiol. 69, 495–503.

Jin, Y.S., Alper, H., Yang, Y.T., Stephanopoulos, G., 2005. Improvement of xylose uptake and ethanol production in recombinant *Saccharomyces cerevisiae* through an inverse metabolic engineering approach. Appl. Environ. Microbiol. 71, 8249.

Johansson, B., Christensson, C., Hobley, T., Hahn-Hägerdal, B., 2001. Xylulokinase overexpression in two strains of *Saccharomyces cerevisiae* also expressing xylose reductase and xylitol dehydrogenase and its effect on fermentation of xylose and lignocellulosic hydrolysate. Appl. Environ. Microbiol. 67, 4249–4255.

Johansson, B., Hahn-Hägerdal, B., 2002. The non-oxidative pentose phosphate pathway controls the fermentation rate of xylulose but not of xylose in *Saccharomyces cerevisiae* TMB3001. FEMS Yeast Res. 2, 277–282.

Karhumaa, K., Hahn-Hägerdal, B., Gorwa-Grauslund, M.-F., 2005. Investigation of limiting metabolic steps in the utilization of xylose by recombinant *Saccharomyces cerevisiae* using metabolic engineering. Yeast 22, 359–368.

Karhumaa, K., Wiedemann, B., Hahn-Hagerdal, B., Boles, E., Gorwa-Grauslund, M.F., 2006. Co-utilization of L-arabinose and D-xylose by laboratory and industrial *Saccharomyces cerevisiae* strains. Microb Cell Fact. 5, 18.

Kerstershilderson, H., Callens, M., Vanopstal, O., Vangrysperre, W., Debruyne, C.K., 1987. Kinetic characterization of D-xylose isomerases by enzymatic assays using D-sorbitol dehydrogenase. Enzyme Microb. Technol. 9, 145–148.

Kuyper, M., Harhangi, H., Stave, A., Winkler, A., Jetten, M., Delaat, W., Denridder, J., Opdencamp, H., Vandijken, J., Pronk, J., 2003. High-level functional expression of a fungal xylose isomerase: the key to efficient ethanolic fermentation of xylose by *Saccharomyces cerevisiae*? FEMS Yeast Res. 4, 69–78.

Kuyper, M., Toirkens, M.M.P., Toirkens, M.J., Almering, M.J.H., Winkler, A. a., van Dijken, J.P., Pronk, J.T., 2005a. Metabolic engineering of a xylose-isomerase-expressing *Saccharomyces cerevisiae* strain for rapid anaerobic xylose fermentation. FEMS Yeast Res. 5, 399–409.

Kuyper, M., Toirkens, M.J., Diderich, J. a., Winkler, A. a., van Dijken, J.P., Pronk, J.T., 2005b. Evolutionary engineering of mixed-sugar utilization by a xylose-fermenting *Saccharomyces cerevisiae* strain. FEMS Yeast Res. 5, 925–934.

Madhavan, A., Tamalampudi, S., Srivastava, A., Fukuda, H., Bisaria, V.S., Kondo, A., 2009a. Alcoholic fermentation of xylose and mixed sugars using recombinant *Saccharomyces cerevisiae* engineered for xylose utilization. Appl. Environ. Microbiol. 82, 1037–1047.

Madhavan, A., Tamalampudi, S., Ushida, K., Kanai, D., Katahira, S., Srivastava, A., Fukuda, H., Bisaria, V.S., Kondo, A., 2009b. Xylose isomerase from polycentric fungus Orpinomyces: gene sequencing, cloning, and expression in *Saccharomyces cerevisiae* for bioconversion of xylose to ethanol. Appl. Environ. Microbiol. 82, 1067–1078.

Maris, A.J.A.V., Winkler, A.A., Kuyper, M., Laat, W.T.A.M.D., Dijken, J.P.V., Pronk, J.T., Fleminglaan, A., Delft, A.X., 2007. Development of efficient xylose fermentation in *Saccharomyces cerevisiae*: xylose isomerase as a key component. Adv. Biochem. Eng. Biotechnol. 108, 179–204.

Moes, C.J., Pretorius, I.S., vanZyl, W.H., 1996. Cloning and expression of the *Clostridium thermosulfurogenes* D-xylose isomerase gene (xylA) in *Saccharomyces cerevisiae*. Biotechnol. Lett. 18, 269–274.

Mumberg, D., Muller, R., Funk, M., 1995. Yeast vectors for the controlled expression of heterologous proteins in different genetic backgrounds. Gene 156, 119–122.

Nevoigt, E., 2008. Progress in metabolic engineering of *Saccharomyces cerevisiae*. Microbiol. Mol. Biol. Rev. 72, 379–412.

Ni, H., Laplaza, J.M., Jeffries, T.W., 2007. Transposon mutagenesis to improve the growth of recombinant *Saccharomyces cerevisiae* on D-xylose. Appl. Environ. Microbiol. 73, 2061–2066.

Ohta, K., Hayashida, S., 1983. Role of tween 80 and monoolein in a lipid–sterol–protein complex which enhances ethanol tolerance of sake yeasts. Appl. Environ. Microbiol. 46, 821–825.

Pitkänen, J.-P., Rintala, E., Aristidou, A., Ruohonen, L., Penttilä, M., 2005. Xylose chemostat isolates of *Saccharomyces cerevisiae* show altered metabolite and enzyme levels compared with xylose, glucose, and ethanol metabolism of the original strain. Appl. Environ. Microbiol. 67, 827–837.

Pronk, J.T., 2002. Auxotrophic yeast strains in fundamental and applied research. Appl. Environ. Microbiol. 68, 2095–2100.

Rosa, Karhumaa, Fonseca, K., Violeta, C., Almeida, J.R., Larsson, C.U., Bengtsson, O., Bettiga, M., Hahn-Hägerdal, B., Gorwa-Grauslund, M.F., 2010. Improved xylose and arabinose utilization by an industrial recombinant *Saccharomyces cerevisiae* strain using evolutionary engineering. Biotechnology for Biofuels 3, 13.

Sarthy, A.V., McConaughy, B.L., Lobo, Z., Sundstrom, J.A., Furlong, C.E., Hall, B.D., 1987. Expression of the *Escherichia coli* xylose isomerase gene in *Saccharomyces cerevisiae*. Appl. Environ. Microbiol. 53, 1996–2000.

Sauer, U., 2001. Evolutionary engineering of industrially important microbial phenotypes. Adv. Biochem. Eng. Biotechnol. 73, 129–169.

Shamanna, D.K., Sanderson, K.E., 1979. Uptake and catabolism of D-xylose in *Salmonella typhimurium* Lt2. J. Bacteriol. 139, 64–70.

Sikorski, R.S., Hieter, P., 1989. A system of shuttle vectors and yeast host strains designed for efficient manipulation of DNA in *Saccharomyces cerevisiae*. Genetics 122, 19–27.

Sonderegger, M., Sauer, U., 2003. Evolutionary engineering of *Saccharomyces cerevisiae* for anaerobic growth on xylose. Appl. Environ. Microbiol. 69, 1990–1998.

Sun, H., Treco, D., Schultes, N.P., Szostak, J.W., 1989. Double-strand breaks at an initiation site for meiotic gene conversion. Nature 338, 87–90.

Toivari, M.H., Aristidou, A., Ruohonen, L., Penttila, M., 2001. Conversion of xylose to ethanol by recombinant *Saccharomyces cerevisiae*: importance of xylulokinase (XKS1) and oxygen availability. Metab. Eng. 3, 236–249.

Ulitsky, I., Maron-Katz, A., Shavit, S., Sagir, D., Linhart, C., Elkon, R., Tanay, A., Sharan, R., Shiloh, Y., Shamir, R., 2010. Expander: from expression microarrays to networks and functions. Nat. Protoc. 5, 303–322.

van Maris, A.J. a., Abbott, D. a., Bellissimi, E., van den Brink, J., Kuyper, M., Luttik, M. a.H., Wisselink, H.W., Scheffers, W.A., van Dijken, J.P., Pronk, J.T., 2006. Alcoholic fermentation of carbon sources in biomass hydrolysates by *Saccharomyces cerevisiae*: current status. Antonie van Leeuwenhoek 90, 391–418.

Van Vleet, J.H., Jeffries, T.W., 2009. Yeast metabolic engineering for hemicellulosic ethanol production. Curr. Opin. Biotechnol. 20, 300–306.

Wahlbom, C.F., Cordero Otero, R.R., van Zyl, W.H., Hahn-Hägerdal, B., Jonsson, L.J., 2003. Molecular analysis of a *Saccharomyces cerevisiae* mutant with improved ability to utilize xylose shows enhanced expression of proteins involved in transport, initial xylose metabolism, and the pentose phosphate pathway. Appl. Environ. Microbiol. 69, 740–746.

Walfridsson, M., Bao, X., Anderlund, M., Lilius, G., Bülow, L., Hahn-Hägerdal, B., 1996. Ethanolic fermentation of xylose with *Saccharomyces cerevisiae* harboring the *Thermus thermophilus* xylA gene, which expresses an active xylose (glucose) isomerase. Appl. Environ. Microbiol. 62, 4648–4651.

Wang, B.L., 2009. High Throughput Screen for Cells with High Extracellular Metabolite Consumption—Secretion Rates Using Microfluidic Droplets. Dept. of Chemical Engineering., Vol. Ph. D. Massachusetts Institute of Technology, Cambridge, MA.

Wang, B.L., Zhou, H., Weitz, D.A., Stephanopoulos, G.N., 2008. Microfluidic droplets as nanobioreactors for screening metabolic engineering libraries. In: The AIChE 2008 Annual Meeting, Philadelphia, PA.

Wiedemann, B., Boles, E., 2008. Codon-optimized bacterial genes improve L-arabinose fermentation in recombinant *Saccharomyces cerevisiae*. Appl. Environ. Microbiol. 74, 2043–2050.